Journal of
Mechanics of
Materials and Structures

ANALYSIS OF IMPACT RESPONSE AND DAMAGE IN LAMINATED COMPOSITE SHELL INVOLVING LARGE DEFORMATION AND MATERIAL DEGRADATION

Surendra Kumar

Volume 3, Nº 9 November 2008

mathematical sciences publishers

JOURNAL OF MECHANICS OF MATERIALS AND STRUCTURES
Vol. 3, No. 9, 2008

ANALYSIS OF IMPACT RESPONSE AND DAMAGE IN LAMINATED COMPOSITE SHELL INVOLVING LARGE DEFORMATION AND MATERIAL DEGRADATION

SURENDRA KUMAR

A nonlinear finite element analysis of impact response and impact-induced damage in curved composite laminates subjected to transverse impact by a foreign object is carried out. An eight-noded isoparametric quadrilateral shell element incorporating a nonlinear strain displacement relation due to large deflection is developed based on the total Lagrangian approach. The nonlinear system of equations is solved using a Newton–Raphson incremental-iterative method. Example problems of graphite/epoxy cylindrically curved laminates with different curvature are considered and the influence of geometrical nonlinearity on the impact response and the resulting damage is demonstrated. The concurrent effect of material degradation due to impact damage is also investigated.

1. Introduction

The impact damage tolerance of aircraft structural composite materials is one of the most important design considerations in designing aircraft structures. Accordingly, the understanding of impact response and impact damage mechanisms has drawn the attention of many investigators. A summary of most of the earlier work is reported in [Cantwell and Morton 1991; Abrate 1991; 1994].

In spite of the extensive literature available on the subject, issues associated with complex impact damage phenomena and the effects of several parameters still require further investigation. Most impact problems for laminated plates have been formulated using small deflection theory [Aggour and Sun 1988; Wu and Springer 1988; Choi and Chang 1992; Nosier et al. 1994; Pradhan and Kumar 2000], which is adequate if the impact load is small. However, it is necessary to include the effect of geometric nonlinearity if the laminate undergoes a large deflection. Ambur et al. [1995] have shown that nonlinear effects can be significant for thin plates subjected to low-velocity impact. The inclusion of geometrical nonlinearity in prediction of impact response and damage in thin and moderately thick laminated composites helps in improving the accuracy of the analysis. Chandrashekhara and Schroeder [1995] have studied the impact response of laminated curved shells using a finite element formulation based on Sander's shell theory considering geometric nonlinearity in the sense of the von Karman strains. However, impact damage was not investigated in their study. Kim et al. [1997] and Her and Liang [2004] have studied the effect of curvature on dynamic response and impact damage in cylindrical shells using a 3-D finite element formulation. However, the analyses of both these papers were linear and were based on small deflection theory. The effect of failed laminas on the stiffness of the laminate was also not accounted for in determining the impact response. Ganapathy and Rao [1998] used a 4-noded 48 degree of freedom shell element based

Keywords: finite element analysis, geometric nonlinearity, eight noded quadrilateral shell element, composite shell, impact, material degradation.

on the Kirchhoff-Love thin shell theory in the finite element analysis of cylindrical/spherical shell panels. The authors used a form of classical Hertzian contact law and predicted matrix cracking failure by applying the general Tsai-Wu failure criterion for composite materials. Although geometrical nonlinearity was included, the study assumes that low velocity impact force and deformation can be simulated by a static model and hence does not compute impact response as a function of time. Krishnamurthy et al. [2001] used a shell element based on the Mindlin-Reissener assumptions for transverse shear deformation in their parametric study of laminated cylindrical composite shells. In another paper [Krishnamurthy et al. 2003], the authors extended their work on the impact response of a laminated composite cylindrical shell as well as a full cylinder by incorporating the classical Fourier series method into the finite element formulation and also predicted impact-induced damage deploying the semiempirical damage prediction model of [Choi and Chang 1992]. According to the authors, the Fourier series method, which gives information regarding the natural frequencies of vibration of the impacted structure, provided a proper basis for adopting the appropriate size of the analysis time step. However, the paper doesn't address nonlinear effects. Zhu et al. [2006] incorporated the effects of strain rate dependency and inelastic behavior of matrix material for analyzing the mechanical response of laminated shell. It was shown by the authors that when the rate dependent modulus and inelastic effects are considered, the shell panels have a considerable damping effect. The study was, however, concentrated on the transient response of a laminated shell subjected to a suddenly applied static loading uniformly distributed over the bottom surface of the panel and did not address damage phenomena. More recently, Kumar et al. [2007] have carried out parametric studies on impact response and damage in curved composite laminates using a 3D eight-noded layered brick element with incompatible modes and have investigated the effect of material degradation on both impact response and damage. However, their finite element formulations were based on linear deformation theory.

In the present paper, a nonlinear finite element transient dynamic analysis is carried out to predict the impact response and the impact-induced damage in a laminated composite cylindrical shell subjected to transverse impact by a metallic impactor. An eight-noded isoparametric quadrilateral shell element incorporating geometrical nonlinearity due to a large deflection is implemented based on the total Lagrangian approach. The nonlinear system of equations resulting from the large displacement formulation and nonlinear contact law are simultaneously solved iteratively using a Newton–Raphson method. Example problems of graphite/epoxy cylindrically curved shells with different curvature are considered and the influence of geometrical nonlinearity on the impact response and impact-induced damage is demonstrated. The study also comprises the simultaneous effect of stiffness reduction of the damaged region in the laminate on impact response and the resulting damage as the solution progresses with time.

2. Mathematical formulation

Basic equations. Consider the laminated doubly curved shell shown in Figure 1. The displacement field at any point within the shell, according to a first order shear deformation theory is given by

$$\begin{aligned} u(x, y, z) &= u_0(x, y) + z\varphi_x(x, y), \\ v(x, y, z) &= v_0(x, y) + z\varphi_y(x, y), \\ w(x, y, z) &= w_0(x, y), \end{aligned} \tag{1}$$

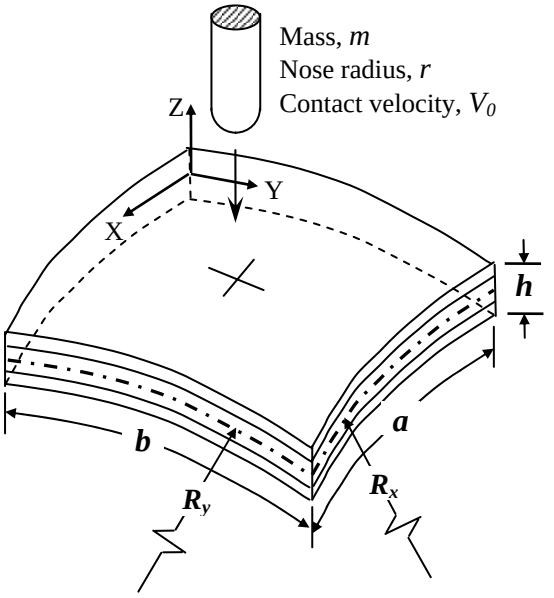

Figure 1. Problem description of impact on a general doubly curved shell.

where u is the membrane displacement in the x-direction, v is the membrane displacement in the y-direction and w is the out-of-plane transverse displacement in the z-direction. u_0, v_0 and w_0 are the midplane displacements. The positive φ_x and φ_y are the cross-sectional clockwise rotations around the y- and x-axes, respectively.

The strain-displacement relations based on Sander's shell theory [1959] and incorporating the geometrical nonlinearity given by [Stein 1986] can be written as

$$\varepsilon_x = \varepsilon_x^0 + z\kappa_x, \quad \varepsilon_y = \varepsilon_y^0 + z\kappa_y, \quad \gamma_{xy} = \gamma_{xy}^0 + z\kappa_{xy}, \quad \gamma_{yz} = \gamma_{yz}^0, \quad \gamma_{xz} = \gamma_{xz}^0, \tag{2}$$

where

$$\begin{aligned}
\varepsilon_x^0 &= \frac{\partial u_0}{\partial x} + \frac{w_0}{R_x} + \frac{1}{2}\left[\left(\frac{\partial u_0}{\partial x}\right)^2 + \left(\frac{\partial v_0}{\partial x}\right)^2 + \left(\frac{\partial w_0}{\partial x} - \frac{u_0}{R_x}\right)^2\right], \\
\varepsilon_y^0 &= \frac{\partial v_0}{\partial y} + \frac{w_0}{R_y} + \frac{1}{2}\left[\left(\frac{\partial u_0}{\partial y}\right)^2 + \left(\frac{\partial v_0}{\partial y}\right)^2 + \left(\frac{\partial w_0}{\partial y} - \frac{v_0}{R_y}\right)^2\right], \\
\gamma_{xy}^0 &= \frac{\partial u_0}{\partial y} + \frac{\partial v_0}{\partial x} + \frac{\partial u_0}{\partial x}\frac{\partial u_0}{\partial y} + \frac{\partial v_0}{\partial x}\frac{\partial v_0}{\partial y} + \left(\frac{\partial w_0}{\partial x} - \frac{u_0}{R_x}\right)\left(\frac{\partial w_0}{\partial y} - \frac{v_0}{R_y}\right)
\end{aligned} \tag{3a}$$

are the nonlinear mid-plane strains,

$$\kappa_x = \frac{\partial \varphi_x}{\partial x}, \quad \kappa_y = \frac{\partial \varphi_y}{\partial y}, \quad \kappa_{xy} = \frac{\partial \varphi_x}{\partial y} + \frac{\partial \varphi_y}{\partial x} + \frac{1}{2}\left(\frac{1}{R_y} - \frac{1}{R_x}\right)\left(\frac{\partial v_0}{\partial x} - \frac{\partial u_0}{\partial y}\right) \tag{3b}$$

are the changes in curvature, and

$$\gamma_{yz}^0 = \varphi_y + \frac{\partial w_0}{\partial y} - \frac{v_0}{R_y}, \quad \gamma_{xz}^0 = \varphi_x + \frac{\partial w_0}{\partial x} - \frac{u_0}{R_x} \tag{3c}$$

are the transverse shear strains. In these equations, R_x and R_y are the radii of curvature in x and y directions. In this equation, higher order terms for the derivatives of cross-sectional rotations and the nonlinear terms in transverse shear strains have been neglected.

If we set

$$\{\bar{\varepsilon}\} = \left[\varepsilon_x^0 \;\; \varepsilon_y^0 \;\; \gamma_{xy}^0 \;\; \kappa_x \;\; \kappa_y \;\; \kappa_{xy} \;\; \gamma_{yz}^0 \;\; \gamma_{xz}^0\right]^T,$$

the laminate constitutive equation can be written as

$$\{F\} = [\bar{D}]\{\bar{\varepsilon}\}, \tag{4}$$

where

$$\{F\} = \left[N_x \;\; N_y \;\; N_{xy} \;\; M_x \;\; M_y \;\; M_{xy} \;\; Q_{yz} \;\; Q_{xz}\right]^T = \left[\int_{-h/2}^{h/2} \left(\sigma_x \;\; \sigma_y \;\; \tau_{xy} \;\; \sigma_x z \;\; \sigma_y z \;\; \tau_{xy} z \;\; \tau_{yz} \;\; \tau_{xz}\right) dz\right]^T \tag{5}$$

is the generalized stress resultant vector[1] and

$$[\bar{D}] = \begin{bmatrix} A_{ij} & B_{ij} & 0 \\ B_{ij} & D_{ij} & 0 \\ 0 & 0 & S_{pq} \end{bmatrix}$$

is the laminate stiffness matrix, with components

$$(A_{ij}, B_{ij}, D_{ij}) = \sum_{k=1}^{N} \int_{z_{k-1}}^{z_k} \bar{C}_{ij}^k (1, z, z^2)\, dz \quad (i, j = 1, 2, 4). \tag{6a}$$

(extensional, bending-stretching coupling and bending stiffness coefficients) and

$$S_{pq} = \sum_{k=1}^{N} \int_{z_{k-1}}^{z_k} \alpha \bar{C}_{pq}^k dz \quad (p, q = 5, 6). \tag{6b}$$

(transverse shear stiffness coefficients). In the last two equations, N is the number of layers, α is the shear correction factor, and $\bar{C}_{ij}^k$ $(i, j = 1, 2, 4, 5, 6)$ represent the transformed elastic constants for the k-th layer, satisfying the relation

$$[\bar{C}] = [T]^T [C][T], \tag{7}$$

where $[T]$ is the transformation matrix relating the strains in the ply principal directions to those in the shell reference axis and $[C]$ is elasticity matrix relating the strains within the ply to the stresses in the ply coordinate system.

Finite element model. Using the principle of virtual work, the equation of equilibrium after including the inertia forces at time t_{n+1} can be given as

$$\{\Psi_{n+1}\} = \iint [B]^T \{F_{n+1}\}\, dx\, dy + \iint [N]^T [P]\{\ddot{u}_{n+1}\}\, dx\, dy - \{R_{n+1}\}, \tag{8}$$

[1]Here N_x, N_y, N_{xy} are the internal in-plane force resultants per unit length, M_x, M_y, M_{xy} are the internal moment resultants and Q_{yz}, Q_{xz} are the transverse shear resultants per unit length.

where $\{\Psi_{n+1}\}$ is residual vector, $[B]$ strain-displacement matrix corresponding to (3a)–(3c), $\{F_{n+1}\}$ is the stress resultant vector at any point, $[N]$ is the shape function matrix, $\{\ddot{u}_{n+1}\}$ is the acceleration vector at any point and $\{R_{n+1}\}$ is the applied load vector. The inertia matrix of the laminate $[P]$ is defined as

$$[P] = \begin{bmatrix} p & 0 & 0 & 0 & 0 \\ 0 & p & 0 & 0 & 0 \\ 0 & 0 & p & 0 & 0 \\ 0 & 0 & 0 & I & 0 \\ 0 & 0 & 0 & 0 & I \end{bmatrix}, \tag{9}$$

with

$$p = \sum_{k=1}^{N} \int_{z_{k-1}}^{z_k} \rho_k dz \quad \text{and} \quad I = \sum_{k=1}^{N} \int_{z_{k-1}}^{z_k} z^2 \rho_k dz, \tag{10}$$

where ρ_k is the mass density of the k-th layer.

In the large displacement problem,

$$[B] = [B_L] + [B_{NL}]$$

and

$$\{F_{n+1}\} = [\bar{D}]\big[[B_L] + \tfrac{1}{2}[B_{NL}]\big]\{U_{n+1}\} = [\bar{D}][\bar{B}]\{U_{n+1}\}, \tag{11}$$

where $[B_L]$ is the contribution from the linear part of the strain and $\frac{1}{2}[B_{NL}]$ is the contribution from the quadratic part of the strain and involves linear functions of the translational components of the element nodal degree of freedom vector $\{U_{n+1}\}$.

In (8),

$$\{\ddot{u}_{n+1}\} = [N]\{\ddot{U}_{n+1}\}. \tag{12}$$

Using the Newmark time integration method with a constant average acceleration ($\alpha = 0.5$ and $\beta = 0.25$), the nodal acceleration vectors $\{\ddot{U}_{n+1}\}$ can be expressed in terms of nodal displacements $\{U_{n+1}\}$ as

$$\{\ddot{U}_{n+1}\} = \frac{1}{\beta(\Delta t)^2}\{U_{n+1}\} - \left(\frac{1}{\beta(\Delta t)^2}\{U_n\} + \frac{1}{\beta(\Delta t)}\{\dot{U}_n\} + \frac{1-2\beta}{2\beta}\{\ddot{U}_n\}\right). \tag{13}$$

Equations (12) and (13) can be put into (8), yielding

$$\{\Psi_{n+1}\} = \iint [B]^T\{F_{n+1}\}\,dx\,dy + \frac{1}{\beta(\Delta t)^2}\left(\iint [N]^T[P][N]\,dx\,dy\right)\{U_{n+1}\} - \{R^M_{n+1}\} - \{R_{n+1}\}. \tag{14}$$

$\{R^M_{n+1}\}$ can be thought of as the load vector due to inertia term at time t_{n+1} and is given by

$$\{R^M_{n+1}\} = [M]\left(\frac{1}{\beta(\Delta t)^2}\{U_n\} + \frac{1}{\beta(\Delta t)}\{\dot{U}_n\} + \frac{1-2\beta}{2\beta}\{\ddot{U}_n\}\right), \tag{15}$$

with $[M] = \iint [N]^T[P][N]\,dx\,dy$ the mass matrix.

In the present analysis, the nonlinear equation (14) is solved iteratively using a Newton–Raphson scheme. It is, therefore, necessary to find the relation between $\{d\Psi_{n+1}\}$ and $\{dU_{n+1}\}$ by taking the variation of the residual force, (14), with respect to $\{U_{n+1}\}$. This relation is

$$[K^T_{n+1}]\,\delta\{U_{n+1}\} = \delta\{\Psi_{n+1}\}, \tag{16}$$

where

$$[K_{n+1}^T] = \iint [B]^T[\bar{D}][B]\,dx\,dy + \iint [G]^T[S_{n+1}][G]\,dx\,dy + \frac{1}{\beta(\Delta t)^2}\left(\iint [N]^T[P][N]\,dx\,dy\right) - \frac{\delta\{R_{n+1}\}}{\delta\{U_{n+1}\}} \quad (17)$$

is the tangent stiffness matrix, in whose expression we have used the following notations:

$$[S] = \begin{bmatrix} N_x[I] & N_{xy}[I] \\ sym & N_y[I] \end{bmatrix}$$

is the matrix of the stress resultant array (with $[I]$ the 3×3 identity matrix), and $[G]$ is matrix of shape function derivatives, defined by

$$\{g_{n+1}\} = [G]\{U_{n+1}\},$$

where

$$\{g\} = \left[\frac{\partial u_0}{\partial x} \quad \frac{\partial v_0}{\partial x} \quad \left(\frac{\partial w_0}{\partial x} - \frac{u_0}{R_x}\right) \quad \frac{\partial u_0}{\partial y} \quad \frac{\partial v_0}{\partial y} \quad \left(\frac{\partial w_0}{\partial y} - \frac{v_0}{R_y}\right)\right]^T.$$

Calculation of contact force. In order to model contact conditions between the impactor and the laminate, the modified version of the Hertzian contact law proposed by [Yang and Sun 1982] based on static indentation tests for cylindrical shell is used in this study. This approach determines the relationship between the contact force, F^c with the indentation depth, α. Since the contact region is generally small in comparison with the dimensions of the shell, the resultant contact force is represented as a point load.

The contact laws as proposed in [Yang and Sun 1982] during loading, unloading and reloading phases are not reproduced here for the sake of brevity; they can be written in a general form as

$$F_{n+1}^c = \phi(\alpha_{n+1}) = \phi(d_{n+1} - w_{n+1}) = \phi\left(d_n + \dot{d}_n\,\Delta t - \frac{1}{4}\frac{F_n^c + F_{n+1}^c}{m}(\Delta t)^2 - w_{n+1}\right), \quad (18)$$

where φ represents a nonlinear relation, d_{n+1} is the displacement of the centre point of the impactor at the $(n+1)$-th time-step and is calculated by applying Newmark's method to the equation of motion of the impactor as in (18). w_{n+1} is the displacement of the mid-surface of the laminate at the impact point in the direction of impact. The last term in (17) consists of dF_{n+1}^c/dw_{n+1}, which can be found by differentiating (18).

Impact damage analysis. It is well known that damage in composite materials is generally complicated consisting of multiple failure modes such as fibre breakage, fibre pullout, matrix cracking, fibre-matrix debonding, delamination between plies, etc. Several investigators have demonstrated that upon impact by a low-velocity projectile, the major part of the damage in the composite laminate is caused by matrix cracking and delamination. Because the tensile failure stress for the fibre is high, damage caused by fibre breakage is generally very limited and confined to the region under and near the contact area between the impactor and the laminate. Based on the experimental observations on low-velocity impact, Choi et al. [1991] reported that intraply matrix cracking is the initial damage mode. Delamination initiates once the matrix crack reaches the interface between the ply groups having different fibre orientations after propagating throughout the thickness of the ply group consisting of the cracked ply. This type of matrix

crack can be referred to as the "critical matrix crack". Several further investigations have indicated that there exists a strong interaction between matrix cracking and delamination and the extent of delamination propagation effectively depends upon the location of matrix cracks.

In the present study, a three-dimensional matrix failure criterion originally proposed in [Hashin 1980] and modified in [Choi et al. 1991] is used. In the latter reference it was shown that there are only three major stresses contributing to transverse matrix cracking in the principal material coordinate system. These are the in-plane transverse normal stress σ_y, the interlaminar transverse shear stress τ_{yz} and the out-of-plane normal stress σ_z. However, the out-of-plane normal stress σ_z is found to be negligibly small compared to the others and decreases rapidly at locations away from the impacted area. Thus, the criterion for the n-th plygroup is simplified as

$$\left(\frac{n_{\bar{\sigma}_y}}{n_Y}\right)^2 + \left(\frac{n_{\bar{\tau}_{yz}}}{n_{S_i}}\right)^2 = e_m^2, \tag{19}$$

where

$$Y = \begin{cases} Y_t & \text{if } \bar{\sigma}_y \geq 0, \\ Y_c & \text{if } \bar{\sigma}_y < 0. \end{cases}$$

In (19), x-y-z is the right-handed ply coordinate system with x-axis representing the fibre direction. $Y_t Y_c$ and S_i are the *in situ* ply transverse tensile strength, *in situ* ply transverse compressive strength and *in situ* interlaminar shear strength respectively within the laminate and e_m is the strength ratio which indicates failure if its value exceeds unity. The bar over the stress components indicates that stresses are averaged within the n-th ply in the thickness direction for predicting the critical matrix cracking.

Although the above equation was proposed in [Choi et al. 1991] for the case of line-loading impact, several further investigators [Choi and Chang 1992; Pradhan and Kumar 2000; Her and Liang 2004; Krishnamurthy et al. 2001; Krishnamurthy et al. 2003; Kumar et al. 2007] assumed this equation to be equally applicable to point-nose impact. However, the present author is of the view that for point-nose impact on curved laminates, the in-plane shear stress τ_{xy} as found in Hashin's matrix failure criterion [1980] must be incorporated in (19) for more accurate estimation.

In (19), *in situ* ply strength refers to the strength of a single ply within a laminate which is considerably different from that measured directly from a unidirectional composite. This difference is generally attributed to the thickness effect of the laminate, adjacent ply constraints and thermal residual stresses [Flaggs and Kural 1982; Peters 1984; Chang and Lessard 1991]. Here empirical relations proposed by [Chang and Lessard 1991] are adopted for calculating *in situ* ply strengths as a function of the laminate thickness and stacking sequence. These relations are given as

$$Y_t = Y_t^0\left(1 + A\frac{\sin(\Delta\theta)}{N^B}\right), \quad S_i = S_{xy}^0\left(1 + C\frac{\sin(\Delta\theta)}{N^D}\right). \tag{20}$$

In (20), Y_t^0 is the transverse tensile strength of a $[90_n]_s$ laminate ($n \geq 6$), S_{xy}^0 is the ply shear strength measured from a unidirectional composite with more than eight layers, $\Delta\theta$ is the minimum ply angle difference between the ply under consideration and its neighbouring plies and N is the number of consecutive plies of the same ply angle. A, B, C and D are material parameters determined from experiment [Chang and Lessard 1991].

A semiempirical criterion to estimate the extent of delamination in composite was proposed in [Choi and Chang 1992], which is based on major stresses attributed to delamination formation. However, the present paper is focussed only on the prediction of critical matrix cracking, since geometrical nonlinearity and the material degradation concept used here will have similar effects on both critical matrix cracking and delamination.

Material degradation concept. Once the critical matrix cracking is predicted at any point within a particular ply group of the shell using the criterion (19), the load carrying capability of the shell decreases. This stiffness loss must be taken into account before the solution proceeds further. Two strategies can be applied to describe the postfailure behaviour of the material. One option is to assume that material fails instantaneously and stiffness values in the corresponding directions are immediately set to zero. Another approach is to use a postfailure model such as those reported in [Ladevèze and LeDantec 1992; Matzenmiller et al. 1995; Johnson et al. 2001; Iannucci and Willows 2006] based on continuum damage mechanics approach. This postfailure model characterizes the growth of damage by a gradual decrease in the corresponding stiffness values using some damage evolution parameter until they reach a final value of zero. It is obvious that, this damage model will provide considerable improvement in the prediction of damage as compared to the instantaneous failure model particularly for the impact of high velocity ranges. This approach may also reduce or eliminate nodal oscillations which may occur in the case of instantaneous failure because of the sudden release of finite amounts of energy. However, this modelling strategy has an inherent complexity in implementation and requires knowledge of the energy dissipation process as a function of the damage mode and its propagation, which must be determined experimentally for a specific damage mode.

For the sake of simplicity, the instantaneous failure model is adopted in the present analysis and the constitutive relation for the damaged element is modified by the use of the reduced material properties such as the one reported in [Choi et al. 1991]. This reduced elastic property matrix can be modified for the present shell element as given below:

$$[C_{\text{red}}] = \begin{bmatrix} E_x & 0 & 0 & 0 & 0 \\ 0 & 0 & 0 & 0 & 0 \\ 0 & 0 & G_{xy} & 0 & 0 \\ 0 & 0 & 0 & 0 & 0 \\ 0 & 0 & 0 & 0 & G_{zx} \end{bmatrix}. \tag{21}$$

Equation (21) is derived based on the reasoning that the damaged region within the element cannot endure any additional in-plane transverse tensile stress and interlaminar transverse shear stress due to the presence of the matrix crack. In order to take into account the partial failure of the element within a ply group, the $[C]$ matrix is replaced by the $[C_{\text{red}}]$ matrix in (7) during Gaussian integration only for those gauss points of the ply group in the element where the failure criterion is satisfied.

This simplified instantaneous stiffness reduction method is reasonable for low-velocity impact in the sense that a general tool is always sought for to predict the combined effect of various damage modes on the performance of the composite structure with complex geometry and loading conditions. Further, this approach will generally not lead to a singularity of the global finite element stiffness matrix, since in the 2D shell element formulation, the whole thickness of the laminate is analysed as an aggregate. For

the same reason, the nodal oscillations will be much less prominent as compared to three-dimensional finite element solutions. Further, stiffness modifications on a gauss point basis will partly ensure gradual stiffness reduction of failed elements.

3. Numerical results and discussions

The above nonlinear finite element formulation was implemented in a specially developed computer code and successfully validated with existing numerical solutions available in literature.

Having validated the present approach, some example problems of T300/976 graphite/epoxy laminated cylindrical shells with different curvatures have been considered to study the impact behaviour of curved composite laminate. Effects of geometrical nonlinearity and material degradation on impact response and resulting damage are also investigated. The problem description of impact on a general doubly curved shell is also depicted in Figure 1. The impacted side is the first layer in the stacking sequence.

Validation problem: Impact response of a rectangular glass/epoxy laminated plate. A square E-glass epoxy cross-ply [0/90/0] laminated plate with a side length of 140 mm and thickness 4.29 mm clamped around the four edges is analyzed. The impactor is a blunt-ended steel circular cylinder having diameter 9.525 mm, length 25.4 mm and mass 0.01417 kg and traveling at an initial velocity of 22.6 ms^{-1}. The material properties of the 1002E-glass epoxy are taken as follows:

$$E_x = 40.0\,\mathrm{GPa}, \quad E_y = E_z = 8.27\,\mathrm{GPa}, \quad G_{xy} = G_{xz} = 4.13\,\mathrm{GPa}, \quad G_{yz} = 0.03\,\mathrm{GPa},$$
$$\nu_{xy} = \nu_{yz} = \nu_{xz} = 0.25, \quad \rho = 1901.5\,\mathrm{kg\,m}^{-3}.$$

The linear and nonlinear solutions of the plate central transverse deflection as a function of time have been compared in Figure 2 with experimental results from [Takeda et al. 1981] and finite element results from [Aggour and Sun 1988]. Good agreement is observed between the present result and the numerical

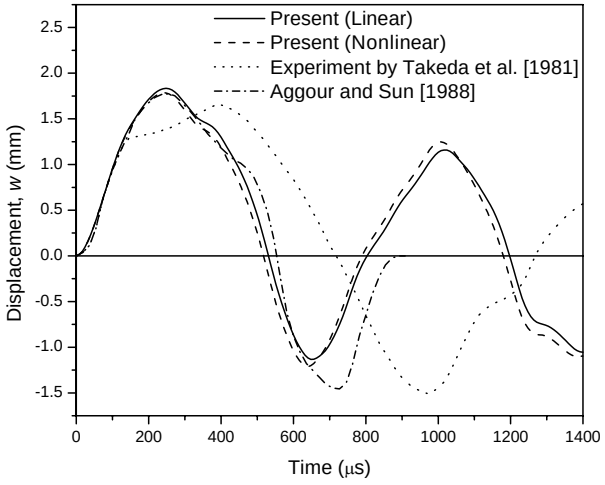

Figure 2. Comparison of plate central transverse deflection in a 140 mm × 140 mm × 4.29 mm E-glass epoxy cross-ply laminate with clamped edges and impacted by 14.175 gm steel projectile at a velocity of 22.6 ms^{-1}.

result. The reasons of discrepancy between numerical and experimental results were well explained in [Aggour and Sun 1988]. It is also apparent from the figure that nonlinear effect is not significant in this case mainly because the plate central deflection is considerably less than the plate thickness.

Validation problem: Clamped [0/90] asymmetric cross-ply cylindrical shell panel subjected to uniform load. As an example of large deflection of composite shell, the asymmetric cross-ply cylindrical shell panel investigated in [Reddy and Chandrashekhara 1985] is considered. The radius and length of the cylindrical shell panel are 64.5 m and 12.9 m respectively. The angle subtended by the arc is 0.2 radian. The thickness of the shell is 64.5 mm. The material properties used are:

$$E_x = 172\,\text{GPa}, \quad E_y = E_z = 7\,\text{GPa}, \quad G_{xy} = G_{yz} = G_{xz} = 3.5\,\text{GPa}, \quad \nu_{xy} = \nu_{yz} = \nu_{xz} = 0.25.$$

The load-deflection curve of the nonlinear solution is given in Figure 3 along with the results of the [Reddy and Chandrashekhara 1985]. Fairly good agreement is seen.

Impact response. T300/976 Graphite/epoxy cylindrical shells of different dimensions and curvatures with $[90_4/0_8/90_4]$ lay-up are considered. At first, $[90_4/0_8/90_4]$ cylindrical shell is taken with $a = b = 300\,\text{mm}$, $R_x = R = 10a$, and $R_y = \infty$ in Figure 1. The shell is clamped on its edges and is subjected to impact by a steel mass of 300 gm having a half sphere head of 10 mm diameter and initial velocity $7\,\text{ms}^{-1}$. The material property data of fiberite T300/976 graphite/epoxy composite are considered as follows [Choi and Chang 1992]:

- Material constants: ply thickness = 0.14224 mm, $\rho = 1540\,\text{kg m}^{-3}$, $E_x = 156\,\text{GPa}$, $E_y = E_z = 9.09\,\text{GPa}$, $G_{xy} = G_{xz} = 6.96\,\text{GPa}$, $G_{yz} = 3.24\,\text{GPa}$, $\nu_{xy} = \nu_{xz} = 0.228$, $\nu_{yz} = 0.4$.
- Lamina strengths: $Y_t^0 = 45\,\text{MPa}$, $Y_c = 252\,\text{MPa}$, $S_{xy}^0 = 105\,\text{MPa}$.
- Empirical parameters: $A = 1.3$, $B = 0.7$, $C = 2.0$, $D = 1.0$.

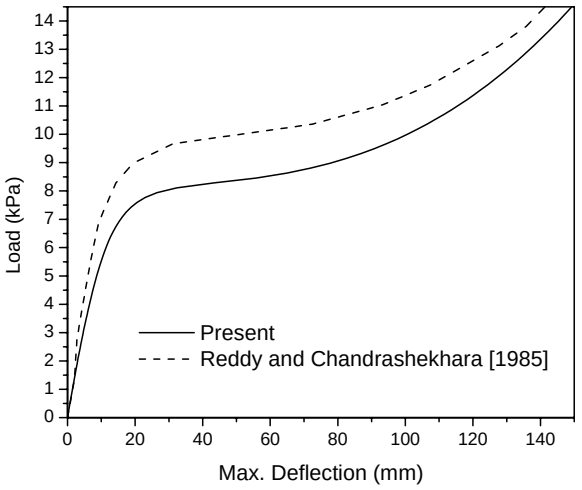

Figure 3. Load-deflection curve for clamped [0/90] asymmetric cross-ply cylindrical shell panel subjected to uniform load.

The results of contact force, impactor displacement and shell centre displacement are presented in Figure 4 for both linear and nonlinear analyses. A reduction in maximum contact force and increase in contact duration and maximum central deflection is observed in the nonlinear solution of the shell with curvature $R = a$ when compared with linear results. Although the peak contact force also increased in the nonlinear solution of shell with curvature $R = 10a$, the contact duration and the maximum shell deflection decreased significantly. The effect of shell curvature is also shown in the Figure. Both the contact duration and the amplitude of shell response decrease with decrease in the shell radius indicating that increasing the curvature has a stiffening effect on the cylindrical shell. However, the results signify that a nonlinear approach has caused a reduction in flexural rigidity of the shell having higher stiffness due to curvature while this has resulted in an increase in flexural rigidity of the shell having lower curvature-induced stiffness.

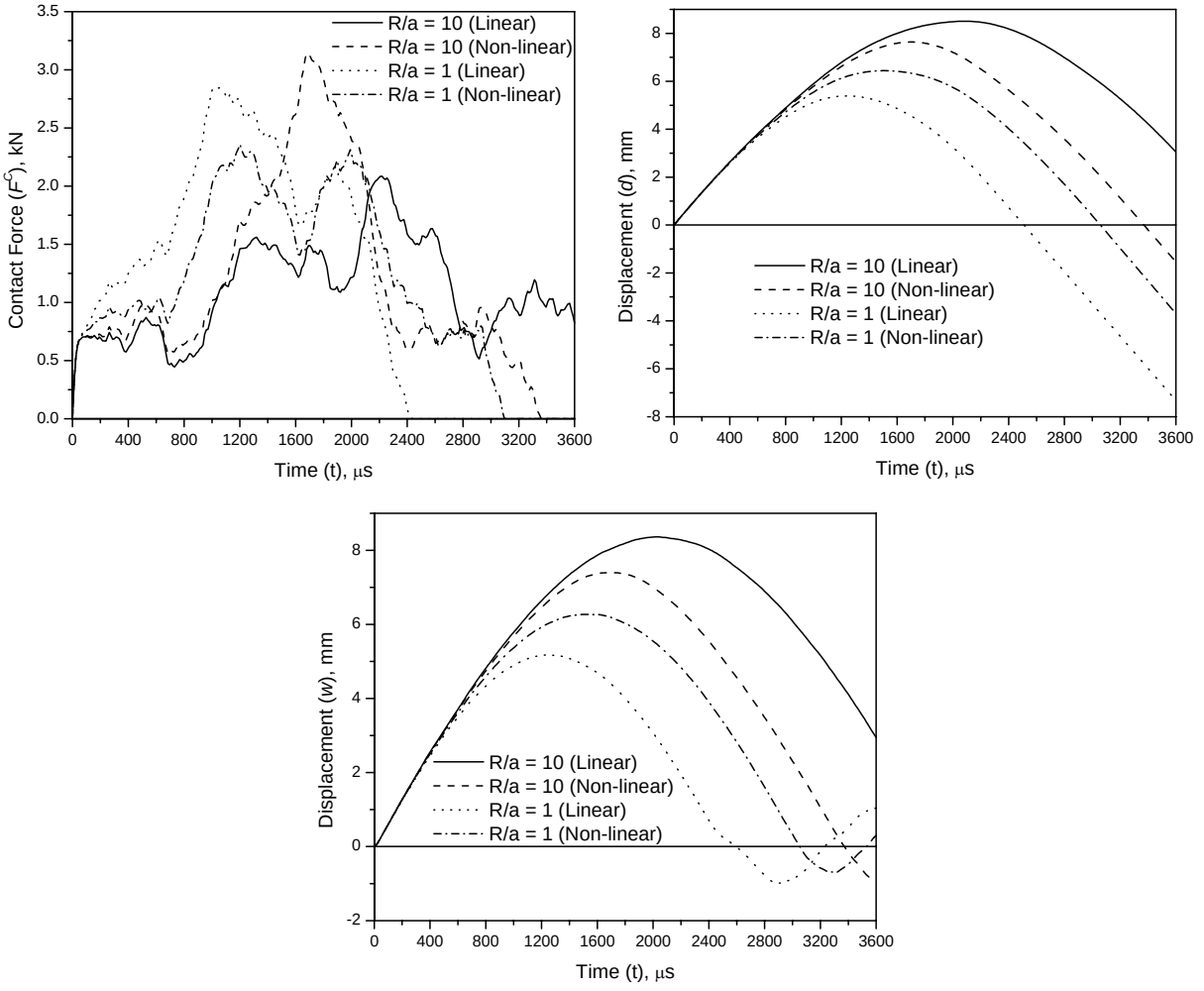

Figure 4. Contact force, impactor displacement and centre displacement in graphite/epoxy cylindrical shells ($[90_4/0_8/90_4]$) ($a = b = 300$ mm; $R = 10a$ and $R = a$), with clamped edges and impacted by blunt-ended steel cylinder of nose radius 5 mm and mass 300 gm having initial velocity of 7 ms^{-1}.

Impact-induced damage. The impact-induced damage in the form of critical matrix cracking is studied for the above cylindrical shell. The shell with $[90_4/0_8/90_4]$ lay-up with dimensions $a = b = 300\,\text{mm}$ and curvature $R = a$ is subjected to an impact by a steel mass of 300 gm and nose radius 5 mm traveling at a velocity of $7\,\text{ms}^{-1}$. Critical matrix cracking takes place in the bottom $[90_4]$ ply group as shown in Figure 5. The value of strength ratio, e_m (critical matrix cracking failure criterion) at any point in the shell is found to be maximum in the bottom $[90_4]$ ply group at time approximately 1056 μs in case of linear analysis and 1212 μs in case of nonlinear analysis. The region where e_m is greater than or equal to unity represents the location of the critical matrix cracking. The failure contour is extended much wider along the fibre direction of the cracked $[90_4]$ ply group than in the direction normal to the fibre direction. Considerable changes in failure profile and a small increase in the damage region are observed in the case of the nonlinear solution even if the maximum contact force was lower as compared to the linear result (Figure 4). This occurs mainly because in the nonlinear case both the bending deformation and hence the bending stress are higher which significantly contributes to matrix cracking. Though the damage primarily occurs near the impact site, the figure indicates that for clamped shell panels damage can also evolve near the boundaries.

Material degradation effects. The effect of reducing the stiffness of damaged elements within the laminas concurrently while computing the impact response and damage is also studied. For this case, a $[90_4/0_8/90_4]$ layup cylindrical shell of dimensions $a = b = 100\,\text{mm}$ and curvature $R = a$ is taken. The impactor is a steel mass of 200 gm having a half sphere head of 10 mm diameter and initial velocity $5\,\text{ms}^{-1}$. The nonlinear results of contact force, impactor displacement and shell center deflection are plotted in Figure 6 for both the cases in which the reduction of stiffness was considered and was not considered. There is a sizeable reduction in peak contact force and increase in both contact duration and maximum shell deflection indicating that overall stiffness of the laminate has reduced considerably when material degradation is incorporated in the solution. The value of the strength ratio, e_m at any

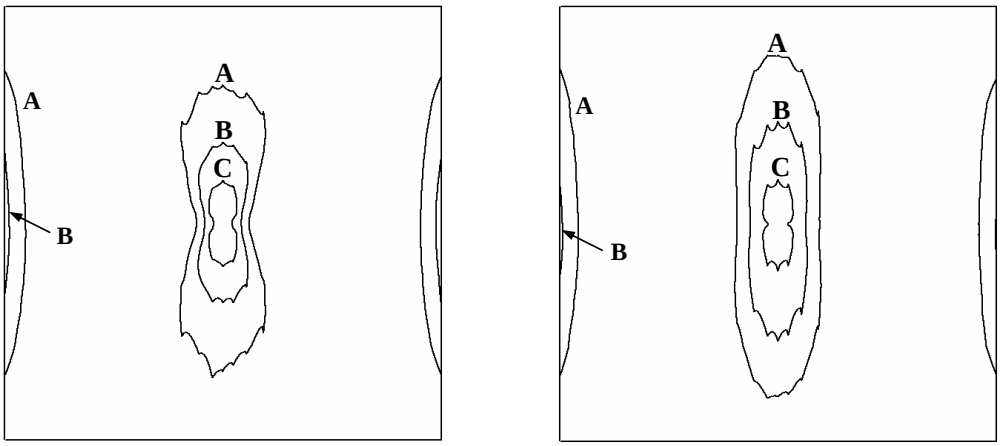

Figure 5. Contours of maximum strength ratio e_m ($A = 0.2$, $B = 0.5$, $C = 1.0$) in bottom $[90_4]$ ply of $[90_4/0_8/90_4]$ lay-up cylindrical shell (dimensions: $a = b = 300\,\text{mm}$; $R = a$) with clamped edges and impacted by a 300 gm mass at a velocity of $7\,\text{ms}^{-1}$. Left: linear analysis; right: nonlinear analysis.

point in the shell is found to be a maximum at approximately 472 μs in case of unmodified stiffness and at approximately 608 μs in case of modified stiffness. The critical matrix cracking profile is plotted in Figure 7 for both the cases. A comparison of the two halves of the figure indicates that the critical matrix cracking has further extended in the direction of the fibre and has reduced in the direction normal to the fibre direction due to material degradation. This is mainly because loads that were sustained by the elements prior to damage are consequently transferred to adjacent elements. It is obvious that this stiffness modification concept will give better results and smooth failure contours with increasing mesh density and decreasing analysis time-step as appropriate.

Although it would be more appropriate to present some sample results depicting improvements brought by incorporating material degradation effects in the finite element solution, an indirect estimation can

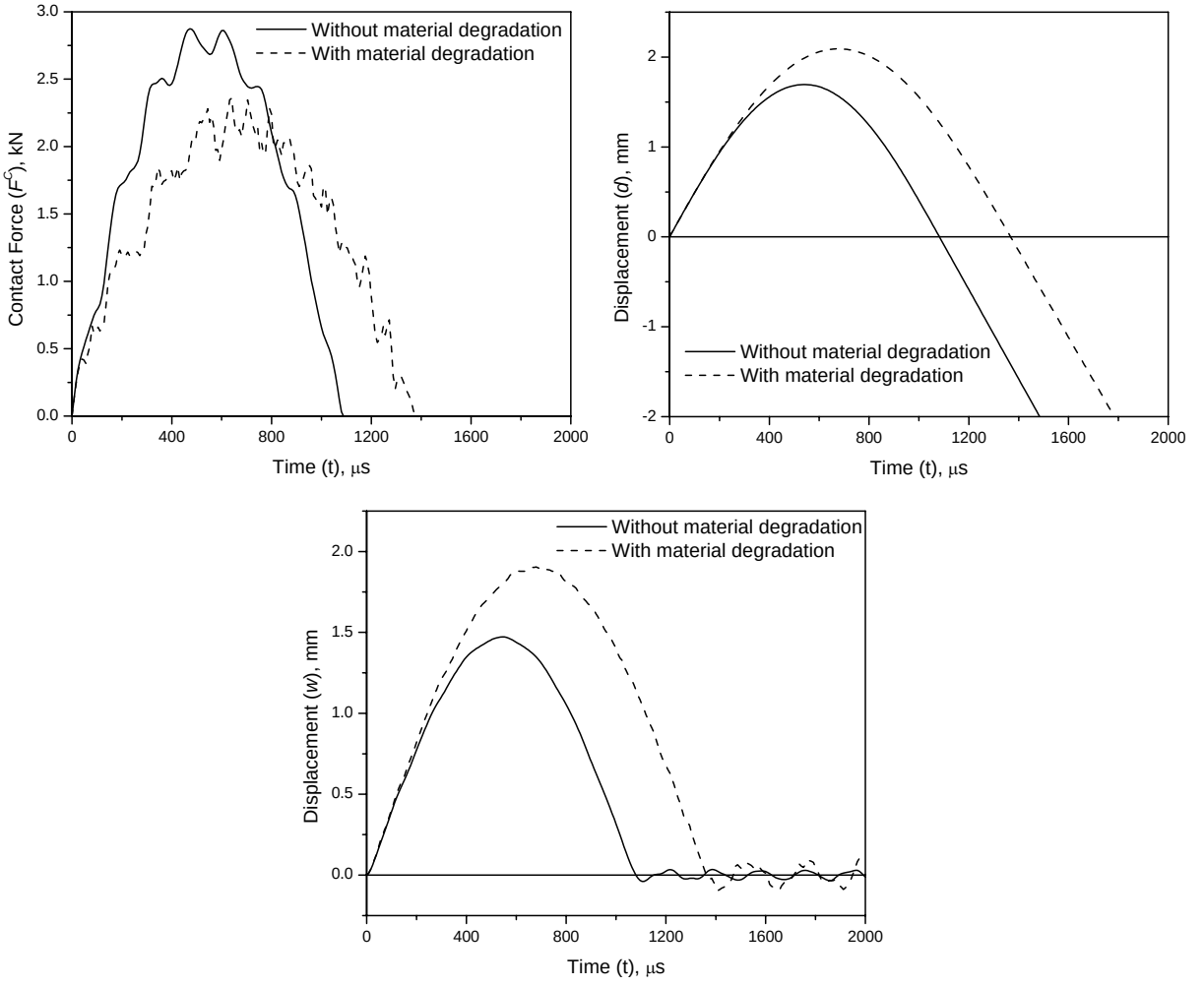

Figure 6. Effect of material degradation on contact force, impactor displacement and centre deflection in graphite/epoxy cylindrical shell ($[90_4/0_8/90_4]$ lay-up) ($a = b = 100$ mm; $R = a$; nonlinear analysis), with clamped edges and impacted by blunt-ended steel cylinder of nose radius 5 mm and mass 200 gm having initial velocity of 5 ms^{-1}.

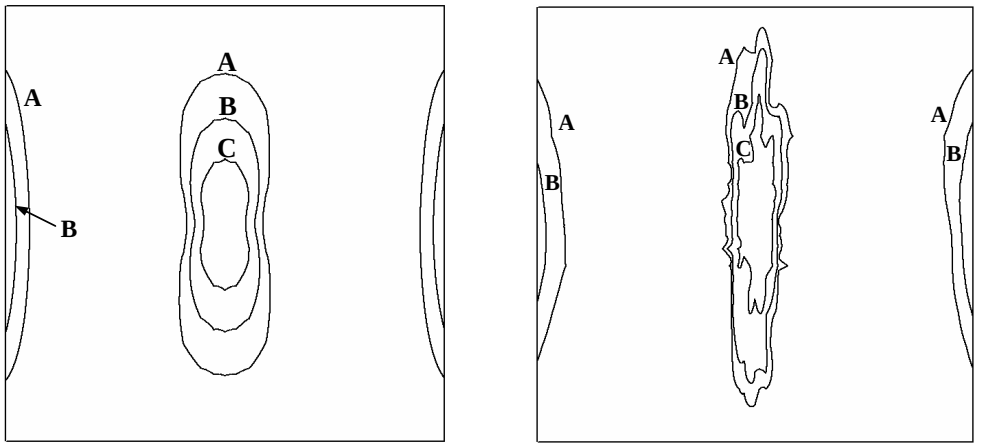

Figure 7. Effect of material degradation on maximum strength ratio e_m ($A = 0.2$, $B = 0.5$, $C = 1.0$) in bottom [90_4] ply of [$90_4/0_8/90_4$] lay-up cylindrical shell (dimensions: $a = b = 300$ mm; $R = a$) with clamped edges and impacted by a 200 gm mass at a velocity of 5 ms^{-1}. Left: without material degradation; right: with material degradation.

be made with regard to the verification problem of Figure 2. One of the reasons cited in [Aggour and Sun 1988] for the inconsistency between numerical and experimental results in Figure 2 was that as the contact time between impactor and plate increases, the failure in the form of matrix cracking and delamination may have started in the laminate reducing its overall stiffness and natural frequency. As in Figure 6, it is expected that if the material degradation concept is integrated in the solution of problem of Figure 2, the contact duration will increase and the mismatch between finite element result and experimental observation will reduce considerably.

4. Conclusion

A finite element and transient dynamic analysis of laminated composite cylindrical shells subjected to transverse impact has been performed using a nonlinear finite element shell formulation and implemented by a specially developed computer code. The tangent stiffness matrix accounting for the geometric nonlinearity is formulated using a generalized Green's strain tensor. The nonlinear system of equations was solved using a Newton–Raphson incremental-iterative method by considering suitable displacement and force convergence norms. Some numerical examples of graphite/epoxy laminated cylindrical shells have been considered with different curvature and nonlinear geometrical effects on impact response and the resulting damage has been studied. Some example problems are also considered in which the stiffness of the failed elements within the laminate is concurrently reduced to account for their loss of load-carrying capability due to matrix cracking. The following are some important observations made from the present study:

1. When the geometrical nonlinearity was included, considerable changes in the time-variation of contact force, impactor displacement and shell deflection occurred for the problems considered. This difference in impact response is found to be significantly dependent on the shell curvature considered.

2. Although damage primarily occurs near the impact site, damage can also evolve near the boundaries for clamped shell panels. A considerable change in the critical matrix cracking profile is noticed when a nonlinear approach is used in the solution.
3. The material property degradation approach used here is found to provide reasonable results and can be easily implemented in cases when a general tool is required to predict the combined effect of various damage modes on the performance of the composite structure with complex geometry and loading conditions.
4. When the stiffness of the failed region is reduced, there is a sizeable reduction in peak contact force in combination with increase in both contact duration and maximum shell deflection. Owing to material property degradation, the shape and extent of critical matrix cracking is noticeably changed extending largely in fibre direction while shrinking in the direction normal to the fibre direction of the cracked ply-group.

Acknowledgement

The author expresses sincere thanks to Dr. A. R. Upadhya, Scientist-In-Charge, CSIR Centre for Mathematical Modelling and Computer Simulation (C-MMACS) for kind permission in publication of the manuscript. He is also thankful to Dr. T. R. Ramamohan, Scientist-G, C-MMACS for suggesting some corrections in the paper.

References

[Abrate 1991] S. Abrate, "Impact on laminated composite materials", *Appl. Mech. Rev.* (*ASME*) **44** (1991), 155–190.

[Abrate 1994] S. Abrate, "Impact on laminated composites recent advances", *Appl. Mech. Rev.* (*ASME*) **47** (1994), 517–544.

[Aggour and Sun 1988] H. Aggour and C. T. Sun, "Finite element analysis of a laminated composite plate subjected to circularly distributed central impact loading", *Comput. Struct.* **28**:6 (1988), 729–736.

[Ambur et al. 1995] D. R. Ambur, J. H. Starnes, Jr., and C. B. Prasad, "Low-speed impact damage-initiation characteristics of selected laminated composite plates", *AIAA J.* **33**:10 (1995), 1919–1925.

[Cantwell and Morton 1991] W. J. Cantwell and J. Morton, "The impact resistance of composite materials: a review", *Composites* **22**:5 (1991), 347–362.

[Chandrashekhara and Schroeder 1995] K. Chandrashekhara and T. Schroeder, "Nonlinear impact analysis of laminated cylindrical and doubly curved shells", *J. Compos. Mater.* **29**:16 (1995), 2160–2179.

[Chang and Lessard 1991] F. K. Chang and L. B. Lessard, "Damage tolerance of laminated composites containing an open hole and subjected to compressive loading, I: Analysis", *J. Compos. Mater.* **25** (1991), 2–43.

[Choi and Chang 1992] H. Y. Choi and F.-K. Chang, "A model for predicting damage in graphite/epoxy laminated composites resulting from low-velocity point impact", *J. Compos. Mater.* **26**:14 (1992), 2134–2169.

[Choi et al. 1991] H. Y. Choi, H. Y. T. Wu, and F. K. Chang, "A new approach towards understanding damage mechanisms and mechanics of laminated composites due to low-velocity impact, II: Analysis", *J. Compos. Mater.* **25** (1991), 1012–1038.

[Flaggs and Kural 1982] D. L. Flaggs and M. H. Kural, "Experimental determination of the in situ transverse lamina strength in graphite/epoxy laminates", *J. Compos. Mater.* **16**:2 (1982), 103–116.

[Ganapathy and Rao 1998] S. Ganapathy and K. P. Rao, "Failure analysis of laminated composite cylindrical/spherical shell panels subjected to low-velocity impact", *Comput. Struct.* **68**:6 (1998), 627–641.

[Hashin 1980] Z. Hashin, "Failure criteria for unidirectional fibre composites", *J. Appl. Mech.* (*ASME*) **47** (1980), 329–334.

[Her and Liang 2004] S.-C. Her and Y.-C. Liang, "The finite element analysis of composite laminates and shell structures subjected to low velocity impact", *Compos. Struct.* **66**:1-4 (2004), 277–285.

[Iannucci and Willows 2006] L. Iannucci and M. L. Willows, "An energy based damage mechanics approach to modelling impact onto woven composite materials, I: Numerical models", *Compos. A Appl. Sci. Manuf.* **37**:11 (2006), 2041–2056.

[Johnson et al. 2001] A. F. Johnson, A. K. Pickett, and P. Rozycki, "Computational methods for predicting impact damage in composites structures", *Compos. Sci. Technol.* **61**:15 (2001), 2183–2192.

[Kim et al. 1997] S. J. Kim, N. S. Goo, and T. W. Kim, "The effect of curvature on the dynamic response and impact-induced damage in composite laminates", *Compos. Sci. Technol.* **57**:7 (1997), 763–773.

[Krishnamurthy et al. 2001] K. S. Krishnamurthy, P. Mahajan, and R. K. Mittal, "A parametric study of the impact response and damage of laminated cylindrical composite shells", *Compos. Sci. Technol.* **61**:12 (2001), 1655–1669.

[Krishnamurthy et al. 2003] K. S. Krishnamurthy, P. Mahajan, and R. K. Mittal, "Impact response and damage in laminated composite cylindrical shells", *Compos. Struct.* **59**:1 (2003), 15–36.

[Kumar et al. 2007] S. Kumar, B. N. Rao, and B. Pradhan, "Effect of impactor parameters and laminate characteristics on impact response and damage in curved composite laminates", *J. Reinf. Plast. Compos.* **26**:13 (2007), 1273–1290.

[Ladevèze and LeDantec 1992] P. Ladevèze and E. LeDantec, "Damage modelling of the elementary ply for laminated composites", *Compos. Sci. Technol.* **43**:3 (1992), 257–267.

[Matzenmiller et al. 1995] A. Matzenmiller, J. Lubliner, and R. L. Taylor, "A constitutive model for anisotropic damage in fibre-composites", *Mech. Mater.* **20**:2 (1995), 125–152.

[Nosier et al. 1994] A. Nosier, R. K. Kapania, and J. N. Reddy, "Low-velocity impact of laminated composites using a layerwise theory", *Comput. Mech.* **13**:5 (1994), 360–379.

[Peters 1984] P. W. M. Peters, "The strength distribution of 90° plies in 0/90/0 graphite-epoxy laminates", *J. Compos. Mater.* **18**:6 (1984), 545–556.

[Pradhan and Kumar 2000] B. Pradhan and S. Kumar, "Finite element analysis of low-velocity impact damage in composite laminates", *J. Reinf. Plast. Compos.* **19**:4 (2000), 322–339.

[Reddy and Chandrashekhara 1985] J. N. Reddy and K. Chandrashekhara, "Nonlinear analysis of laminated shells including transverse shear strains", *AIAA J.* **23**:3 (1985), 440–441.

[Sanders 1959] J. L. Sanders, Jr., "An improved first-approximation theory for thin shells", Technical report R–24, NASA, 1959, Available at http://www.ntis.gov/search/product.aspx?ABBR=PB175839.

[Stein 1986] M. Stein, "Nonlinear theory for plates and shells including the effects of transverse shearing", *AIAA J.* **24**:9 (1986), 1537–1544.

[Takeda et al. 1981] N. Takeda, R. L. Sierakowski, and L. E. Malvern, "Wave propagation experiments on ballistically impacted composite laminates", *J. Compos. Mater.* **15**:2 (1981), 157–174.

[Wu and Springer 1988] H.-S. T. Wu and G. S. Springer, "Impact induced stresses, strains, and delaminations in composite plates", *J. Compos. Mater.* **22**:6 (1988), 533–560.

[Yang and Sun 1982] S. H. Yang and C. T. Sun, "Indentation law for composite laminates", pp. 425–449 in *Composite materials: testing and design* (*6th conference*) (Phoenix, AZ, 1991), edited by I. M. Daniel, ASTM Special Technical Publication **787**, American Society for Testing and Materials, Philadelphia, 1982. Paper ID: STP28494S.

[Zhu et al. 2006] L. Zhu, A. Chattopadhyay, and R. K. Goldberg, "Multiscale analysis including strain rate dependency for transient response of composite laminated shells", *J. Reinf. Plast. Compos.* **25**:17 (2006), 1795–1831.

Received 23 Jul 2008. Revised 2 Nov 2008. Accepted 13 Nov 2008.

SURENDRA KUMAR: surendra@cmmacs.ernet.in
Council of Scientific and Industrial Research, Centre for Mathematical Modelling and Computer Simulation, NAL Belur Campus, Bangalore, Karnataka 560037, India